A current sheet model for the Earth's magnetic field

Daniel R. Stump and Gerald L. Pollack

Citation: **66**, (1998); doi: 10.1119/1.18961
View online: http://dx.doi.org/10.1119/1.18961
View Table of Contents: http://aapt.scitation.org/toc/ajp/66/9
Published by the American Association of Physics Teachers

A current sheet model for the Earth's magnetic field

Daniel R. Stump and Gerald L. Pollack
Department of Physics and Astronomy, Michigan State University, East Lansing, Michigan 48824-1116

(Received 10 November 1997; accepted 10 March 1998)

As an example in magnetostatics we consider the main magnetic field of the Earth and its current sources. The measured field on the surface is accurately given, in tables of the International Geological Reference Field, in terms of Gaussian coefficients. By applying Maxwell's equations to these data we calculate the extended field, inside the Earth, and give graphical representations of it. We also construct a simple theoretical model of the source of the field, in which the field is the result of currents flowing on the surface of a sphere inside the Earth. The current sources which give the observed field are calculated in terms of vector spherical harmonics. The stream function and currents are displayed on a Mercator projection for a sphere whose radius is half the Earth's radius. Interesting properties of vector operations on the Mercator plane are analytically and graphically described.

I. INTRODUCTION

An interesting real magnetic phenomenon is the Earth's magnetic field. In this paper we consider this phenomenon as an example in magnetostatics. We construct a simple theoretical model of the current that produces the field.

Earth's magnetic field, as currently understood by geologists,[1,2] is produced by currents deep in the Earth's interior. Earth's mean radius a is about 6371 km. The currents which are the sources of the geomagnetic field are thought to flow in the Earth's liquid outer core, a conducting liquid consisting mostly of Fe with a few percent Ni and lighter elements. The liquid outer core occupies the region $0.21a \leqslant r \leqslant 0.55a$. The conducting liquid is under high pressure (from 140 GPa at the top to 330 GPa at the bottom), and at high temperature ($\approx 4000 \pm 1000$ °C at the top). Its resistivity, which is not well known, is about $1.7 \times 10^{-6}\ \Omega$m;[1] for comparison the resistivity of Cu at room temperature is $1.7 \times 10^{-8}\ \Omega$m.[3] From the center of the Earth out to $r = 0.21a$, i.e., beneath the liquid outer core, is the inner core, which is a conducting solid with the same composition but at higher pressure and temperature. The region from the top of the liquid outer core to the Earth's surface, called the mantle and crust, consists largely of oxides; it is solid and nonconducting.[4,5]

The actual currents in the liquid outer core are complicated because the driving forces and the fluid flow are complicated. This system is usually treated with dynamo theory, magnetohydrodynamics, and other sophisticated mathematical methods.[6–9] To determine the sources from the observed magnetic field is a difficult inverse problem. Two recent numerical simulations of the geodynamo[8,9] give very useful information, but much remains to be done before we understand it sufficiently.

In this paper we ask: Is there a simple current distribution which would give the observed geomagnetic field? The model we analyze is that the current resides on the surface of a sphere in the Earth's liquid outer core, i.e., it is a spherical current sheet.

Our calculations illustrate basic principles of magnetostatics, vector analysis, and spherical harmonic functions. These are topics that would be included in an undergraduate course on electromagnetism. We remark that problems in magnetic dipole dynamics have pedagogical interest as well, but are usually more advanced.[10–13] One purpose of our paper is to provide a pedagogical example with real physical significance. Although the model is idealized, it does give an interesting qualitative picture of geomagnetism.[14]

We will present our results for fields and currents on a Mercator plane projection of the Earth. In many ways a Mercator plane may be considered to be a Cartesian plane in

which the coordinates are (longitude, latitude), in our notation (ϕ,λ), instead of (x,y). In terms of the azimuthal angle ϕ and the polar angle θ of spherical coordinates we have $(\phi,\lambda)=(\phi,90°-\theta)$. We show in this paper, as an instructional tool, how vector operations in spherical coordinates behave on a Mercator plane.

The plan of the paper is as follows. In Sec. II we describe the observed magnetic field at the surface of the Earth, in terms of an expansion in spherical harmonics. In Sec. III we construct the current sheet model, and relate the surface current density to the exterior field. There is a one-to-one correspondence between the coefficients of the spherical harmonic expansions of the field and the current. In Secs. IV and V we discuss some implications of our model calculations.

In this paper we are concerned with what is called the *main field*, i.e., the intrinsic field due to electric current in the Earth's core. We do not address the question of the origin of the current, which is also a very interesting problem,[2,15] but we do calculate, and display, the current within the idealized model of a current sheet.

II. MAGNETIC FIELD OF THE EARTH

The Earth's magnetic field, at the surface of the Earth, has been measured for centuries. The magnetic compass was invented in China, probably over 2000 years ago, and came to Europe in the 12th century. In 1546, Gerhard Mercator understood from his observations that the point that magnetic needles seek is terrestrial and not in the stars. Ultimately, in 1600, William Gilbert in *De Magnete* described experiments on spherical lodestones from which he concluded that the Earth itself is a great magnet or, as he put it, ''*magnus magnes ipse est globus terrestris*.'' This predates by almost 90 years Newton's understanding of the terrestrial origin of gravity.

The static magnetic field **B**, outside the region of its source currents, satisfies the field equations

$$\nabla\cdot\mathbf{B}=0, \quad \nabla\times\mathbf{B}=0. \tag{1}$$

In this source-free region we may express **B** in terms of either a vector potential **A** or a scalar potential Φ_M. The scalar potential is simpler, so we write

$$\mathbf{B}=-\nabla\Phi_M. \tag{2}$$

By (1) the potential must satisfy Laplace's equation, $\nabla^2\Phi_M=0$.

It is natural to expand $\Phi_M(\mathbf{x})$ in spherical harmonics, an analysis first carried out by Gauss in 1839. The conventional choice of normalization[16] is

$$\Phi_M(\mathbf{x})=a\sum_{\ell=1}^{\infty}\sum_{m=0}^{\ell}\left(\frac{a}{r}\right)^{\ell+1}\times(g_\ell^m\cos m\phi+h_\ell^m\sin m\phi)P_\ell^m(\cos\theta), \tag{3}$$

where a is the radius of the Earth; also, r,θ,ϕ are the polar coordinates of **x** in a coordinate system in which the rotation axis of the Earth is the positive z axis. For the exterior potential the radial dependence of harmonic ℓ is $r^{-\ell-1}$. Gauss's expression for the magnetic scalar potential was essentially the same as (3), except that he included terms only up to $\ell=4$ and used a different normalization. The functions

Table I. Gauss coefficients, in nanoTeslas (nT), for $\ell=1$–3, in the year 1990, from the DGRF.

ℓ	m	g_ℓ^m	h_ℓ^m	ℓ	m	g_ℓ^m	h_ℓ^m
1	0	−29 775	0	3	0	1314	0
1	1	−1 848	5406	3	1	−2239	−284
2	0	−2 131	0	3	2	1248	293
2	1	3 059	−2279	3	3	802	−352
2	2	1 686	−373				

$P_\ell^m(x)$, where x denotes $\cos\theta$, are the associated Legendre functions with the Schmidt normalization

$$\int_{-1}^{1}[P_\ell^m(x)]^2dx=\frac{2}{2\ell+1}(2-\delta(m,0)); \tag{4}$$

in terms of Legendre polynomials $P_\ell(x)$,

$$P_\ell^0(x)=P_\ell(x), \tag{5}$$

$$P_\ell^m(x)=\sqrt{\frac{2(\ell-m)!}{(\ell+m)!}}(1-x^2)^{m/2}\frac{d^mP_\ell}{dx^m} \tag{6}$$

for $m=1,2,3...,\ell$. Note that the spherical harmonic functions used here, i.e., the functions $(\sin m\phi)P_\ell^m(\cos\theta)$ and $(\cos m\phi)P_\ell^m(\cos\theta)$, are real. The sum begins with $\ell=1$ because there is no magnetic monopole, which would correspond to $\ell=0$.

The expansion coefficients g_ℓ^m and h_ℓ^m in (3) are called Gauss coefficients.[17] For each ℓ there are $2\ell+1$ real coefficients. (The coefficient h_ℓ^0 is identically 0.) In our calculations we use the values given in the International Geological Reference Field (IGRF) table of Gauss coefficients.[18] The IGRF tabulation lists the coefficients for ℓ from 1 to 10, averaged over 5-year intervals from 1900 to 1995. The coefficients vary somewhat on a time scale of 5 years, but in this paper we are not concerned with the time dependence of the field. The particular Gauss coefficients we use are those for 1990, called DGRF 1990.[19] Table I gives the values of these coefficients for $\ell=1,2,3$. In our full calculations we use the Gauss coefficients for ℓ from 1 to 8.

A. The dipole component of the field

It is often stated that the magnetic field of the Earth is approximately a dipole field. Later we shall test this statement, but as a first step toward understanding **B** we consider its dipole component. That is, we truncate the sum in (3) at $\ell=1$. In this approximation **B** is identical to the field of a point dipole **m** located at the center of the Earth.

The three Gauss coefficients with $\ell=1$ are related to **m** as follows. Let θ_m,ϕ_m be the polar angles of the dipole axis, with respect to the rotation axis of the Earth; then the Cartesian components of the dipole moment are

$$\mathbf{m}=m(\sin\theta_m\cos\phi_m,\sin\theta_m\sin\phi_m,\cos\theta_m). \tag{7}$$

The scalar potential of the dipole **m** is[20,21]

$$\Phi_d=\frac{\mu_0}{4\pi}\frac{\mathbf{m}\cdot\mathbf{r}}{r^3}=\frac{\mu_0 m}{4\pi r^2}\times[\cos\theta_m\cos\theta+\sin\theta_m\sin\theta\cos(\phi-\phi_m)]. \tag{8}$$

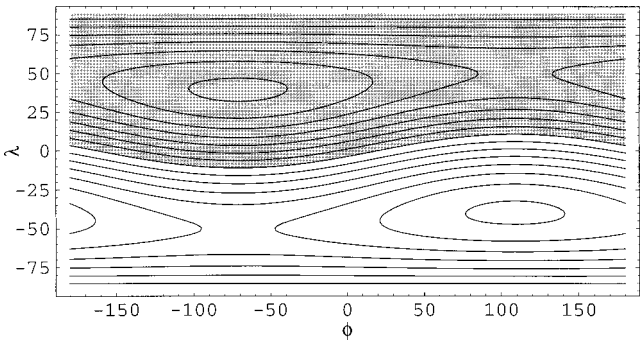

Fig. 1. Contour plot of the dipole component of $B_r \sin\theta$ in the Mercator plane around the Earth's axis of rotation. The abscissa ϕ is the conventional longitude; it is zero at Greenwich and taken positive or negative, respectively, to the east and west. The ordinate λ is the conventional latitude; it is zero at the equator and taken positive or negative, respectively, to the north and south. In the Mercator plane the net flux of $B_r \sin\theta$ is zero. Shaded and unshaded regions are those in which $B_r \sin\theta$ is, respectively, negative and positive. The s-shaped contour between the shaded and unshaded regions is the intersection, with the Earth's surface, of the plane which passes through the center of the Earth and is perpendicular to the magnetic dipole moment. Along that contour, $B_r \sin\theta=0$. At the center of the roughly concentric features in the northern and southern hemispheres $B_r \sin\theta$ is maximum in magnitude. At the geomagnetic poles, which are different points, B_r for the dipole field is maximum in magnitude.

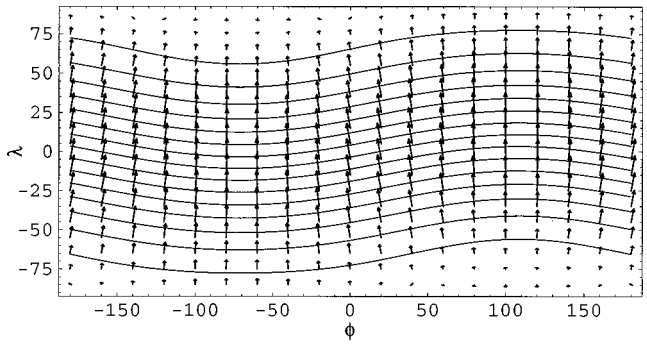

Fig. 2. Contour plot of the dipole component of Φ_M and the tangential field $\mathbf{B}_{\rm Mer}$. This is another representation of the Earth's dipole field in the same Mercator plane as Fig. 1. The solid lines are equipotentials of the magnetic dipole scalar potential. That is, along these lines, Φ_d of (8) is constant, where θ_m and ϕ_m are given in (16) and (17). The arrows show the directions and magnitudes of $\mathbf{B}_{\rm Mer}$, the dipolar magnetic field vector. The (λ,ϕ) coordinates of the geomagnetic north and south poles, discussed in Sec. II A, are, respectively, (79°, −71°) and (−79°, 109°). At these points $\mathbf{B}_{\rm Mer}=0$.

Comparing (3) and (8) we deduce the Gauss coefficients for a point dipole from

$$4\pi a^3 g_1^0 = \mu_0 m \cos\theta_m, \tag{9}$$

$$4\pi a^3 g_1^1 = \mu_0 m \sin\theta_m \cos\phi_m, \tag{10}$$

$$4\pi a^3 h_1^1 = \mu_0 m \sin\theta_m \sin\phi_m. \tag{11}$$

Or, we may invert these equations to determine from the measured Gauss coefficients the equivalent point dipole parameters

$$m = \frac{4\pi a^3}{\mu_0}\sqrt{(g_1^0)^2+(g_1^1)^2+(h_1^1)^2}, \tag{12}$$

$$\cos\theta_m = g_1^0/\sqrt{(g_1^0)^2+(g_1^1)^2+(h_1^1)^2}, \tag{13}$$

$$\tan\phi_m = h_1^1/g_1^1. \tag{14}$$

Using the 1990 DGRF values, and 6371 km as the Earth's radius, (12)–(14) imply that the values of the dipole parameters are

$$m = 7.84\times 10^{22}\ \text{A m}^2, \tag{15}$$

$$\theta_m = 169\ \text{deg}, \tag{16}$$

$$\phi_m = 109\ \text{deg}. \tag{17}$$

The dipole moment is tilted by 169 deg with respect to the Earth's rotation axis, and has azimuthal angle 109 deg. (The zero for azimuthal angles is taken to be the prime meridian, through Greenwich. Positive and negative values of ϕ are, respectively, east and west of Greenwich.) Therefore the points where the dipole component of **B** is normal to the Earth's surface, which are called the geomagnetic north and south poles,[1] are the two antipodal points at (i) latitude 79, longitude −71 (northern hemisphere), and (ii) latitude −79, longitude 109 (southern hemisphere).

Figure 1 shows the normal, i.e., radial component $B_r(\theta,\phi)$ on the surface of the Earth, for the dipole component of the Earth's magnetic field **B**, in the form of a contour plot on a Mercator projection. The abscissa ϕ is the longitude, which is the same as the azimuthal angle. The ordinate λ is the latitude in degrees, and the polar angle θ is $90-\lambda$. The north geographic pole is at $\lambda=90$, the equator is at $\lambda=0$, and the prime meridian is at $\phi=0$. The quantity whose contours are plotted is $B_r(\theta,\phi)\sin\theta$. The factor $\sin\theta$ is included because it is $B_r \sin\theta$ that must integrate to zero on the Mercator plane as can be seen from Gauss's law:

$$\int \nabla\cdot\mathbf{B}\,dV = \int a^2 B_r \sin\theta\, d\theta\, d\phi = 0. \tag{18}$$

Notice in (18) that $a^2 d\theta d\phi = -a^2 d\lambda d\phi$ is an infinitesimal area in the Mercator plane. The relation between λ and θ, namely, $\lambda=90-\theta$, is linear with change of sign. As usual in a Mercator projection, the entire upper boundary is the north pole and the entire lower boundary is the south pole. Figure 1 shows how the magnetic field at the Earth's surface points outward near the south pole, and inward near the north pole. The serpentine shape of the contours shows how the field of a dipole tilted with respect to the axis of projection appears on a Mercator map. If **m** were along the Earth's axis, i.e., along the axis of projection, then we'd have $B_r \sin\theta = (\mu_0 m_0 \sin 2\theta)/4\pi a^3$, which is independent of ϕ. In that case the contours would simply be horizontal lines.

Figure 2 shows the dipole contribution of the tangential vector field $\mathbf{B}_{\rm Mer}=\hat\theta B_\theta+\hat\phi B_\phi \sin\theta$, on the surface of the Earth, in the Mercator plane. In Fig. 2 we have superimposed contours of the Gauss potential Φ_M, which for the dipole case is just Φ_d of (8), and arrows whose direction and length represent the field $\mathbf{B}_{\rm Mer}$. This field is not the same as the magnetic field $\mathbf{B}=-\nabla\Phi_M$ because of the factor $\sin\theta$ in the ϕ component. We plot $\mathbf{B}_{\rm Mer}$ because this field is perpendicular to the contours of Φ_M on a Mercator map. An equivalent definition of $\mathbf{B}_{\rm Mer}$ is

$$\mathbf{B}_{\rm Mer} = -\frac{1}{a}\left(\hat\theta\,\frac{\partial\Phi_M}{\partial\theta}+\hat\phi\,\frac{\partial\Phi_M}{\partial\phi}\right). \tag{19}$$

The right-hand side of (19) is the negative gradient in the Mercator plane. It is formally similar to the negative gradient in a Cartesian plane, but with coordinates (ϕ,θ).

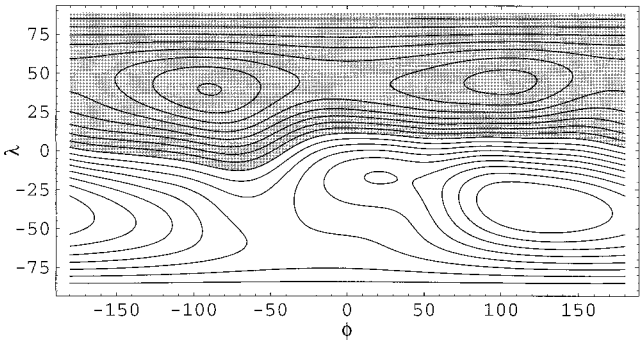

Fig. 3. Contour plot of $B_r \sin\theta$ at $r=a$ for the full normal field. The details are the same as in Fig. 1 except that for these contours all terms from $\ell=1$ through $\ell=8$ have been included. The contour values range from -4×10^4 to 4×10^4 nT.

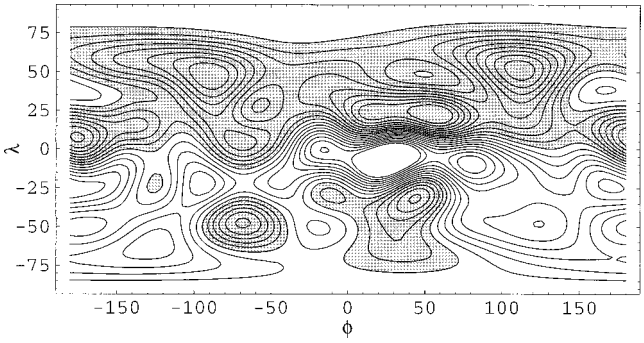

Fig. 5. Contour plot of $B_r \sin\theta$ at $r=a/2$. The details are the same as in Fig. 3 except that in this case the field is shown at half the Earth's radius, i.e., within the liquid outer core. The contour values range from -7.2×10^5 to 7.2×10^5 nT.

B. The full field

Next we consider a more accurate description of the field, based on the Gauss expansion (3) truncated at $\ell=8$. (The DGRF and IGRF tables also include $\ell=9$ and 10, but the coefficients at these high ℓ values are very small, and not so precisely measured as for lower ℓ values, so we have neglected the terms with $\ell>8$. For higher values of ℓ the results are contaminated by contributions of crustal magnetic sources. In Sec. IV we comment on the convergence of the expansion in ℓ.)

Figure 3 shows the full normal field $B_r(\theta,\phi)$, analogous to Fig. 1.

Figure 4 shows the full tangential field $\mathbf{B}_{\rm Mer}=\hat{\theta}B_\theta+\hat{\phi}B_\phi \sin\theta$, analogous to Fig. 2.

These results show that the actual field on the surface differs measurably from a pure dipole field.

C. The field near the source

We may write $\mathbf{B}=-\nabla\Phi_M$ for any points outside the region of the electric currents that are the source of the main field. If we assume that the currents are inside a sphere of radius r_0 then we may use Gauss's potential to calculate $\mathbf{B}$ down to that depth. The contribution from multipole ℓ is proportional to $r^{-\ell-1}$, so the higher multipoles grow in importance as r decreases. The field at r_0 is much different from the surface field at a if r_0 is small compared to a.

We shall plot the magnetic field for $r_0=a/2$, i.e., on a spherical surface within the Earth's liquid outer core, assuming there are no source currents at $r>r_0$. Figure 5 shows the corresponding contours of $B_r \sin\theta$, analogous to Fig. 3 for the surface field. Figure 6 shows the corresponding coutours of Φ_M at $r=r_0=a/2$, and superimposed arrows for the tangential vectors $\mathbf{B}_{\rm Mer}$, analogous to Fig. 4. In Figs. 5 and 6 we again truncate the Gauss expansion in ℓ at $\ell=8$.

Figures 5 and 6 show that the Earth's magnetic field near its source is much different from a pure dipole field. The surface field, which is nearly a dipole field, is only a pale remnant of the complicated field near the source. In our model, and probably for the real field as well, the dipole character of the surface field is really not a defining feature of the Earth's magnetic field, even though it was essential for early seafarers and other explorers. It is rather the result of the rapid decrease with distance from the source, of contributions from multipoles with $\ell\geqslant2$.

III. THE CURRENT SHEET MODEL

As an exercise in magnetostatics, we make a model of the currents inside the Earth which produce the observed field. The model postulates a surface current density $\mathbf{K}(\theta,\phi)$ on the surface of a sphere of radius r_0 inside the Earth. We will characterize this surface current density by the coefficients in an expansion of $\mathbf{K}(\theta,\phi)$ in spherical harmonics. Within the current sheet model we can determine uniquely the connec-

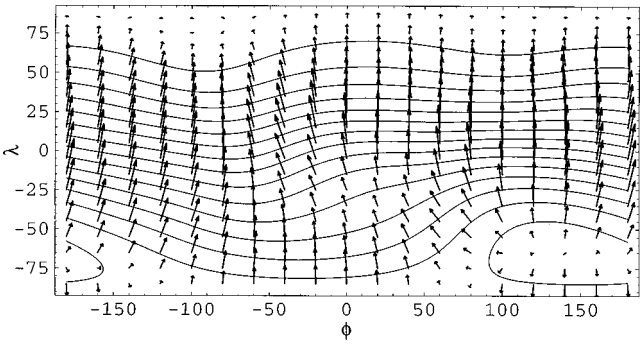

Fig. 4. Contour plot of Φ_M and the tangential field $\mathbf{B}_{\rm Mer}$ at $r=a$ for the full field. The details are the same as in Fig. 2 except that for these contours all terms from $\ell=1$ through $\ell=8$ have been included. The surveyed ($\sim$1990) locations of the North and South Magnetic Poles (or dip poles) where the observed magnetic field is perpendicular to Earth's surface are, approximately, (78.5°, −103.4°) near Ellef Ringnes Island, Canada, and (−65°, 139°) in Commonwealth Bay, Antarctica, given as (λ,ϕ) coordinates. At those points $\mathbf{B}_{\rm Mer}$ is essentially zero.

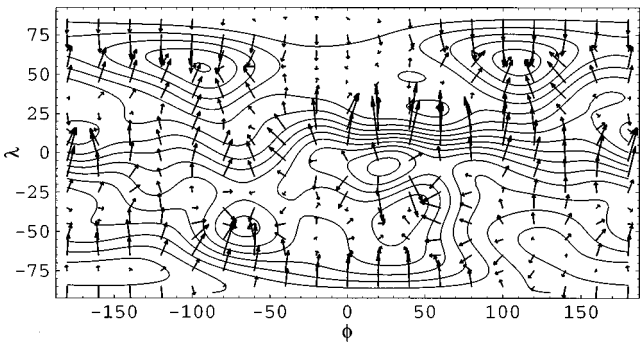

Fig. 6. Contour plot of Φ_M and the tangential field $\mathbf{B}_{\rm Mer}$ at $r=a/2$. The details are the same as in Fig. 4 except that in this case the field is shown at half the Earth's radius.

tion between these surface current coefficients and the Gauss coefficients g_ℓ^m and h_ℓ^m,[18] which we used to describe the Earth's magnetic potential in (3). There will be a one-to-one correspondence between the Gauss coefficients and the current coefficients.

It is important to keep in mind that this is an idealized, naive, model of the actual currents, but it has the advantage that one can examine its consequences in quantitative detail, as we will see. The insights obtained may be useful in examining the effect on the Earth's magnetic field of the real currents as more is learned about them in the future.

A. Derivations

Consider a surface current $\mathbf{K}$ on the surface of a sphere of radius r_0. A general surface current can be written in the form

$$\mathbf{K}(\theta,\phi)=\sum_{\ell=1}^{\infty}\sum_{m=-\ell}^{\ell}K_{\ell m}\mathbf{L}Y_{\ell m}(\theta,\phi), \tag{20}$$

where $Y_{\ell m}$ denotes the complex spherical harmonics. In (20) the spherical harmonics $Y_{\ell m}(\theta,\phi)$ and coefficients $K_{\ell m}$ are complex. The function $\mathbf{K}(\theta,\phi)$ is real, so the complex coefficients $K_{\ell m}$ are chosen such that the imaginary part of (20) is zero. [A purely real expansion for $\mathbf{K}(\theta,\phi)$ is given in (35).] Here $\mathbf{L}$ is the differential operator $\mathbf{x}\times\boldsymbol{\nabla}$; i.e.,

$$\mathbf{L}=\mathbf{x}\times\boldsymbol{\nabla}=\hat{\phi}\,\frac{\partial}{\partial\theta}-\frac{\hat{\theta}}{\sin\,\theta}\,\frac{\partial}{\partial\phi}. \tag{21}$$

The functions $\mathbf{L}Y_{\ell m}$ are called *vector spherical harmonics*.[20,22] Vector spherical harmonics are discussed in Sec. 16.2 of Ref. 20 and in Sec. 9.2 of Ref. 22. The representation (20) is in terms of a *scalar stream function* ψ: $\mathbf{K}$ is $\mathbf{x}\times\boldsymbol{\nabla}\psi$ where $\psi=\Sigma_{\ell=1}^{\infty}\Sigma_{m=-\ell}^{\ell}K_{\ell m}Y_{\ell m}$. Note that the divergence of $\mathbf{K}$ is 0 as it must be because the current is conserved and does not vary with time

$$\begin{aligned}\boldsymbol{\nabla}\cdot\mathbf{K}&=\frac{1}{r_0\,\sin\,\theta}\left[\frac{\partial}{\partial\theta}\,(K_\theta\,\sin\,\theta)+\frac{\partial}{\partial\phi}\,K_\phi\right]\\&=\frac{1}{r_0\,\sin\,\theta}\left[-\frac{\partial}{\partial\theta}\frac{\partial\psi}{\partial\phi}+\frac{\partial}{\partial\phi}\frac{\partial\psi}{\partial\theta}\right]=0.\end{aligned} \tag{22}$$

Outside of the sphere of radius r_0 the magnetic field may be written as $\mathbf{B}=-\boldsymbol{\nabla}\Phi_M$. We now proceed to relate the Gauss coefficients of Φ_M, defined in (3), to the current coefficients $K_{\ell m}$.

The vector potential. We have, where $\mathbf{x}$ is the field point and $\mathbf{x}'$ is the source point,[20,21]

$$\begin{aligned}\mathbf{A}(\mathbf{x})&=\frac{\mu_0}{4\pi}\int\frac{\mathbf{K}da'}{|\mathbf{x}-\mathbf{x}'|}\\&=\frac{\mu_0}{4\pi}\sum_{\ell=1}^{\infty}\sum_{m=-\ell}^{\ell}K_{\ell m}\int\frac{\mathbf{L}'Y_{\ell m}(\Omega')r_0^2d\Omega'}{|\mathbf{x}-\mathbf{x}'|}.\end{aligned} \tag{23}$$

Use the *addition theorem*,[23] for $r>r'=r_0$,

$$\frac{1}{|\mathbf{x}-\mathbf{x}'|}=\sum_{\lambda=0}^{\infty}\sum_{\mu=-\lambda}^{+\lambda}\frac{4\pi}{2\lambda+1}\,\frac{r_0^\lambda}{r^{\lambda+1}}\,Y_{\lambda\mu}(\Omega)Y_{\lambda\mu}^*(\Omega') \tag{24}$$

so $\mathbf{A}(\mathbf{x})$ has the expansion

$$\begin{aligned}\mathbf{A}(\mathbf{x})=&\sum_{\ell=1}^{\infty}\sum_{m=-\ell}^{\ell}K_{\ell m}\sum_{\lambda=0}^{\infty}\sum_{\mu=-\lambda}^{+\lambda}\frac{\mu_0r_0^{\lambda+2}}{(2\lambda+1)r^{\lambda+1}}\,Y_{\lambda\mu}(\Omega)\\&\times\int Y_{\lambda\mu}^*(\Omega')\mathbf{L}'Y_{\ell m}(\Omega')d\Omega'.\end{aligned} \tag{25}$$

Now, in (25) the integral over $d\Omega'$ is zero unless $\lambda=\ell$; therefore we may replace λ by ℓ in the factor $r_0^{\lambda+2}/(2\lambda+1)r^{\lambda+1}$, without changing the value of the right-hand side of (25). After that replacement, that factor can be taken outside the sum over λ, so

$$\begin{aligned}\mathbf{A}(\mathbf{x})=&\sum_{\ell=1}^{\infty}\sum_{m=-\ell}^{\ell}K_{\ell m}\frac{\mu_0r_0^{\ell+2}}{(2\ell+1)r^{\ell+1}}\sum_{\lambda=0}^{\infty}\sum_{\mu=-\lambda}^{+\lambda}Y_{\lambda\mu}(\Omega)\\&\times\int Y_{\lambda\mu}^*(\Omega')\mathbf{L}'Y_{\ell m}(\Omega')d\Omega'.\end{aligned} \tag{26}$$

Now insert the *completeness relation* of spherical harmonics,

$$\sum_{\lambda=0}^{\infty}\sum_{\mu=-\lambda}^{+\lambda}Y_{\lambda\mu}(\Omega)Y_{\lambda\mu}^*(\Omega')=\delta(\phi-\phi')\,\delta(\cos\,\theta-\cos\,\theta'), \tag{27}$$

and use the delta functions to evaluate the integral over $d\Omega'$. The result is

$$\mathbf{A}(\mathbf{x})=\sum_{\ell=1}^{\infty}\sum_{m=-\ell}^{\ell}K_{\ell m}\frac{\mu_0r_0^{\ell+2}}{(2\ell+1)r^{\ell+1}}\,\mathbf{L}Y_{\ell m}(\Omega). \tag{28}$$

Equation (28) is, finally, the vector potential in terms of the coefficients $K_{\ell m}$.

The scalar potential. The problem now is to connect the current coefficients $K_{\ell m}$ with the scalar potential Φ such that $\boldsymbol{\nabla}\times\mathbf{A}=-\boldsymbol{\nabla}\Phi$. To solve this problem we have the following lemma.

Lemma. If $\mathbf{A}=\mathbf{L}Y_{\ell m}/r^{\ell+1}$ then $\boldsymbol{\nabla}\times\mathbf{A}=-\boldsymbol{\nabla}\Phi$ where $\Phi=-\ell Y_{\ell m}/r^{\ell+1}$.

To prove the lemma, first note that

$$\mathbf{A}=\frac{\mathbf{L}Y_{\ell m}}{r^{\ell+1}}=\frac{1}{r^{\ell+1}}\left[\hat{\phi}\,\frac{\partial Y_{\ell m}}{\partial\theta}-\frac{\hat{\theta}}{\sin\,\theta}\,\frac{\partial Y_{\ell m}}{\partial\phi}\right]. \tag{29}$$

Because $Y_{\ell m}\propto e^{im\phi}$ we may replace $\partial/\partial\phi$ by im. Now calculate the curl of $\mathbf{A}$. It is straightforward, using the properties of the spherical harmonics, to show that

$$\boldsymbol{\nabla}\times\mathbf{A}=\ell\boldsymbol{\nabla}\left(\frac{Y_{\ell m}}{r^{\ell+1}}\right)=-\boldsymbol{\nabla}\Phi, \tag{30}$$

where Φ is as given in the lemma.

By applying the Lemma to each term in (28), we have the following expression for the scalar potential:

$$\Phi_M=-\sum_{\ell=1}^{\infty}\sum_{m=-\ell}^{\ell}K_{\ell m}\,\frac{\mu_0r_0^{\ell+2}}{2\ell+1}\,\frac{\ell Y_{\ell m}}{r^{\ell+1}}. \tag{31}$$

Relating the expansion coefficients. We have been using the complex spherical harmonic functions $Y_{\ell m}$. To make the connection to the Gauss expansion, we must now rewrite the result in terms of the associated Legendre functions with the Schmidt normalization. The spherical harmonics are

$$Y_{\ell 0}=\sqrt{\frac{2\ell+1}{4\pi}}\,P_\ell^0(\cos\,\theta), \tag{32}$$

$$Y_{\ell m}=\sqrt{\frac{2\ell+1}{8\pi}}\,(-1)^m P_\ell^m(\cos\,\theta)e^{im\phi}, \tag{33}$$

where $m=1,2,...,\ell$; and $Y_{\ell,-m}=(-1)^m Y^*_{\ell m}$.

The next step is to write an expansion of the surface current $\mathbf{K}$ in real form. We have, in terms of the complex spherical harmonics,

$$\mathbf{K}=\mathbf{L}\sum_{\ell=1}^{\infty}\left\{K_{\ell 0}Y_{\ell 0}+\sum_{m=1}^{\ell}\,(K_{\ell m}Y_{\ell m}+K_{\ell,-m}Y_{\ell,-m})\right\}, \tag{34}$$

which can be reexpressed in terms of real functions as

$$\mathbf{K}=\sum_{\ell=1}^{\infty}\sum_{m=0}^{\ell}\,[k_{\ell m}^{(1)}\mathbf{L}P_\ell^m\,\cos\,m\phi+k_{\ell m}^{(2)}\mathbf{L}P_\ell^m\,\sin\,m\phi] \tag{35}$$

where

$$k_{\ell 0}^{(1)}=K_{\ell 0}\sqrt{(2\ell+1)/4\pi}, \tag{36}$$

$$k_{\ell 0}^{(2)}=0, \tag{37}$$

$$k_{\ell m}^{(1)}=(K_{\ell m}(-1)^m+K_{\ell,-m})\sqrt{(2\ell+1)/8\pi}, \tag{38}$$

$$k_{\ell m}^{(2)}=i(K_{\ell m}(-1)^m-K_{\ell,-m})\sqrt{(2\ell+1)/8\pi}. \tag{39}$$

Notice that in (35) the sum over m is from zero to ℓ.

Finally, in a similar way, we rewrite the expansion of Φ_M in (31) in terms of real variables, and so relate the Gauss coefficients to the current coefficients $k_{\ell m}^{(1)}$ and $k_{\ell m}^{(2)}$; the result is[7,17]

$$g_\ell^m=-\frac{\mu_0\ell}{2\ell+1}\left(\frac{r_0}{a}\right)^{\ell+2}k_{\ell m}^{(1)}, \tag{40}$$

$$h_\ell^m=-\frac{\mu_0\ell}{2\ell+1}\left(\frac{r_0}{a}\right)^{\ell+2}k_{\ell m}^{(2)}. \tag{41}$$

We use (40) and (41) to calculate the current coefficients of our model from the measured Gauss coefficients.

B. Result of the model

One use to which the above formalism can be put is to make a picture of the surface currents which must flow on a sphere of a given radius in order to produce the **B** field which is observed at Earth's surface. For the radius of this sphere we choose $r_0=a/2$.

The current is shown in Fig. 7 in the following way. Equation (35), together with (21), shows that $\mathbf{K}$ may be represented in terms of the scalar stream function $\psi(\theta,\phi)$ as $\mathbf{K}=\mathbf{x}\times\nabla\psi(\theta,\phi)$ where, in terms of real variables,

$$\psi(\theta,\phi)=\sum_{\ell=1}^{\infty}\sum_{m=0}^{\ell}\,[k_{\ell m}^{(1)}\,\cos\,m\phi+k_{\ell m}^{(2)}\,\sin\,m\phi]P_\ell^m(\cos\,\theta). \tag{42}$$

In Fig. 7, the solid curves are contours of $\psi(\theta,\phi)$ shown in the Mercator plane. Superimposed on these are arrows which represent the vector field of the current flow $\mathbf{K}_{\rm Mer}=\hat\theta K_{{\rm Mer},\theta}+\hat\phi K_{{\rm Mer},\phi}=\hat\theta K_\theta\,\sin\,\theta+\hat\phi K_\phi$. This tangential vector differs from $\mathbf{K}$, by the factor $\sin\,\theta$ in the θ component. We construct $\mathbf{K}_{\rm Mer}$ to be tangent to the streamlines in the Mercator plane: we require $\mathbf{K}_{\rm Mer}\cdot\nabla_{\rm Mer}\psi=K_{{\rm Mer},\theta}(\partial\psi/\partial\theta)+K_{{\rm Mer},\phi}(\partial\psi/\partial\phi)=0$. But from $K_\theta=(-1/\sin\,\theta)(\partial\psi/\partial\phi)$ and $K_\phi=(\partial\psi/\partial\theta)$ it follows that $K_{{\rm Mer},\theta}=K_\theta\,\sin\,\theta$ and $K_{{\rm Mer},\phi}=K_\phi$. We remark that the gradient of ψ in the Mercator plane, $\nabla_{\rm Mer}\psi=\hat\theta(\partial\psi/\partial\theta)+\hat\phi(\partial\psi/\partial\phi)=\hat\lambda(\partial\psi/\partial\lambda)+\hat\phi(\partial\psi/\partial\phi)$, has the same form with respect to angular coordinates as the gradient in a Cartesian plane has with respect to linear coordinates. In calculating ψ and $\mathbf{K}_{\rm Mer}$ for Fig. 7 we again used the 1990 DGRF Gauss coefficients for ℓ from 1 to 8.[18]

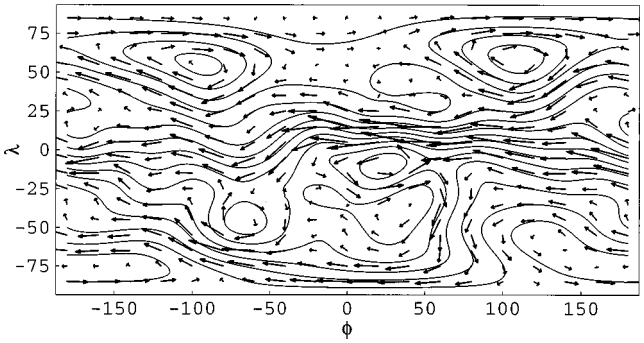

Fig. 7. The model surface currents which flow on a spherical sheet at $r=a/2$, displayed as a contour plot of the stream function $\psi(\theta,\phi)$ and the tangential current field in a Mercator plane. The arrows represent the surface current vector $\mathbf{K}_{\rm Mer}=\hat\theta K_\theta\,\sin\,\theta+\hat\phi K_\phi=-\hat\theta(\partial\psi/\partial\phi)+\hat\phi(\partial\psi/\partial\theta)$. This is perpendicular to $\nabla_{\rm Mer}\psi=\hat\theta(\partial\psi/\partial\theta)+\hat\phi(\partial\psi/\partial\phi)$. Therefore, the arrows are tangent to the contours of ψ.

C. The field for $r<r_0$, and the discontinuity at the current sheet

Taking the current sheet model seriously, we can also determine the field inside the current sheet, i.e., for $r<r_0$. This region is source free, so again we may write $\mathbf{B}=-\nabla\Phi_i$ and expand the interior potential Φ_i in spherical harmonics

$$\Phi_i=a\sum_{\ell=1}^{\infty}\sum_{m=0}^{\ell}\left(\frac{r}{a}\right)^\ell\times[g_{i\ell}^m\,\cos\,m\phi+h_{i\ell}^m\,\sin\,m\phi]P_\ell^m(\cos\,\theta). \tag{43}$$

For the interior potential, the radial form of harmonic ℓ is r^ℓ. To determine the interior coefficients $g_{i\ell}^m$ and $h_{i\ell}^m$ we use the fact that the normal component of $\mathbf{B}$ must be continuous across the current sheet; here the normal direction is radial, so the continuity condition is

$$\frac{\partial\Phi_i}{\partial r}=\frac{\partial\Phi_M}{\partial r} \tag{44}$$

at $r=r_0$. Comparing the coefficients of $\cos\,m\phi P_\ell^m$ and $\sin\,m\phi P_\ell^m$ on the left and right sides of (44) we find that the interior Gauss coefficients are

$$g_{i\ell}^m=-\left(\frac{\ell+1}{\ell}\right)\left(\frac{a}{r_0}\right)^{2\ell+1}g_\ell^m, \tag{45}$$

$$h_{i\ell}^m=-\left(\frac{\ell+1}{\ell}\right)\left(\frac{a}{r_0}\right)^{2\ell+1}h_\ell^m. \tag{46}$$

An interesting point about this result is the *sign change* from g_ℓ^m and h_ℓ^m to $g_{i\ell}^m$ and $h_{i\ell}^m$. The direction of the tangential field inside the current sheet is *opposite* to that outside.

The normal component of **B** is continuous at the current sheet, but the tangential components are discontinuous, with the discontinuity proportional to the surface current[20,21]

$$\lim_{\epsilon\to 0}[\mathbf{B}(r_0+\epsilon)-\mathbf{B}(r_0-\epsilon)]=\mu_0(\mathbf{K}\times\hat{r}). \tag{47}$$

This relation provides another way to derive the surface current **K**. As before, we may express **K** in terms of the stream function ψ, as $\mathbf{K}=\mathbf{x}\times\nabla\psi$. Then the components of (47) are

$$-\frac{1}{r_0}\left(\frac{\partial\Phi_M}{\partial\theta}-\frac{\partial\Phi_i}{\partial\theta}\right)=\mu_0\frac{\partial\psi}{\partial\theta}, \tag{48}$$

$$-\frac{1}{r_0\sin\theta}\left(\frac{\partial\Phi_M}{\partial\phi}-\frac{\partial\Phi_i}{\partial\phi}\right)=\frac{\mu_0}{\sin\theta}\frac{\partial\psi}{\partial\phi}, \tag{49}$$

which are satisfied if

$$-\frac{1}{r_0}(\Phi_M-\Phi_i)=\mu_0\psi. \tag{50}$$

It follows that the spherical harmonic expansion of the stream function is given by (42) where

$$k_{\ell m}^{(1)}=\frac{-1}{\mu_0 r_0}\left\{\frac{a^{\ell+2}}{r_0^{\ell+1}}g_\ell^m-\frac{r_0^\ell}{a^{\ell-1}}g_{i\ell}^m\right\}, \tag{51}$$

$$k_{\ell m}^{(2)}=\frac{-1}{\mu_0 r_0}\left\{\frac{a^{\ell+2}}{r_0^{\ell+1}}h_\ell^m-\frac{r_0^\ell}{a^{\ell-1}}h_{i\ell}^m\right\}. \tag{52}$$

Finally, we may use (45) and (46) to substitute for the interior coefficients. This substitution yields the relation between the current coefficients $k_{\ell m}^{(1)}$ and $k_{\ell m}^{(2)}$ and the exterior Gauss coefficients g_ℓ^m and h_ℓ^m, and the result is identical to the relations (40) and (41) derived earlier.

IV. ENERGY CONSIDERATIONS

A. Field energy

As shown in Fig. 6 the field near the source is qualitatively more complex than the field at the surface, which is predominantly a dipole field. To make this statement quantitative, it is interesting to consider the energy density associated with different harmonics as a function of depth.[24]

The volume energy density is

$$u(\mathbf{x})=\frac{\mathbf{B}^2}{2\mu_0}=\frac{(\nabla\Phi_M)^2}{2\mu_0}. \tag{53}$$

The *radial energy density* (energy per unit radius) is defined as

$$u_r(r)=\int u(\mathbf{x})r^2d\Omega. \tag{54}$$

We may express $u_r(r)$ in terms of the Gauss coefficients.

Let $U(R)$ be the total field energy in the region $r\geqslant R$,

$$U(R)=\int_{r\geqslant R}u(\mathbf{x})d^3x=\int_R^\infty u_r(r)dr. \tag{55}$$

Then $u_r(R)=-dU/dR$. To calculate $U(R)$ we can use a trick. We have

$$U(R)=\int_{r\geqslant R}\frac{(\nabla\Phi_M)^2}{2\mu_0}d^3x. \tag{56}$$

Table II. Contributions to the radial energy density from different spherical harmonics at the Earth's surface ($r=a$) and at $r=a/2$, which is assumed to be outside the source currents. We have taken $a=6371.2$ km. The units are 10^{10} J/m.

ℓ	$u_\ell(a)$	$u_\ell(a/2)$
1	37.3	597
2	1.34	86
3	0.749	192
4	0.206	211
5	0.041	168
6	0.010	163
7	0.003	202
8	0.0004	114

Now write $(\nabla\Phi_M)^2$ as $\nabla\cdot(\Phi_M\nabla\Phi_M)-\Phi_M\nabla^2\Phi_M$; the second term is 0 for r outside of the current, and the first term can be integrated by Gauss's law, with the result

$$U(R)=\frac{-R^2}{2\mu_0}\int\Phi_M\frac{\partial\Phi_M}{\partial R}d\Omega. \tag{57}$$

Substituting the Gauss expansion for Φ_M, and using the orthogonality relations, we find[17]

$$U(R)=\frac{4\pi a^3}{2\mu_0}\sum_{\ell=1}^\infty\frac{\ell+1}{2\ell+1}\left(\frac{a}{R}\right)^{2\ell+1}\sum_{m=0}^\ell[(g_\ell^m)^2+(h_\ell^m)^2]. \tag{58}$$

Thus, finally, since $u_r=-dU/dR$, the radial energy density at radius R is

$$u_r(R)=\frac{4\pi a^2}{2\mu_0}\sum_{\ell=1}^\infty(\ell+1)\left(\frac{a}{R}\right)^{2\ell+2}\sum_{m=0}^\ell[(g_\ell^m)^2+(h_\ell^m)^2]. \tag{59}$$

In order to identify how much of the energy is in the ℓth harmonic of the field we write

$$u_r(r)=\sum_{\ell=1}^\infty u_\ell(r), \tag{60}$$

where $u_\ell(r)$ is the contribution to the radial energy density from the ℓ spherical harmonics. Table II shows $u_\ell(a)$, the ℓ dependence of radial energy density at the Earth's surface; and $u_\ell(a/2)$, the ℓ dependence at the current source, assumed again to be at radius $r_0=a/2$. At the surface, the dipole term ($\ell=1$) dominates; but near the source, the higher multipoles are significant. Indeed, even multipoles with $\ell>8$ are presumably important, because $u_8(a/2)$ is larger than $u_2(a/2)$.

Table II shows that $u_\ell(a/2)$ does not decrease significantly with ℓ as ℓ increases from 1 to 8: At $r=a/2$ the multipole expansion converges very slowly. For larger values of r, e.g., for $r=a$, the convergence is more rapid because of the factor $(a/r)^{2\ell+2}$. (For $r>\sim 0.6a$ the expansion converges reasonably well with $\ell\leqslant 8$.) We have truncated the expansion at $\ell=8$ because the Gauss coefficients are measured accurately for $\ell\leqslant 8$; for higher ℓ values the accuracy is less, because their contribution at $r=a$ is very small, and contaminated by crustal magnetic sources. The fact that large ℓ values are important at the depth of the liquid core implies that the source current varies significantly on small

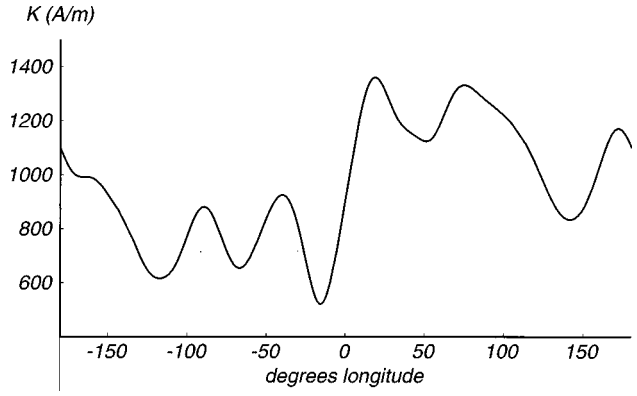

Fig. 8. The magnitude of the surface current along the equator of a sphere whose radius is half of Earth's radius.

length scales, having even smaller scale features than the current shown in Fig. 7 from unmeasured contributions with $\ell > 8$.

B. Power dissipated in resistance

As a final point of discussion, we estimate the power dissipated in electrical resistance, based on the results of our simple current sheet model.

Figure 8 shows the magnitude K of the current density $\mathbf{K}$ for points along the equator, $\lambda = 0$, at depth $r_0 = a/2$. The graph shows that the order of magnitude of K is 10^3 A/m in this model. We may use this value of K to estimate the order of magnitude of the power that must be supplied to maintain the magnetic field.

In our idealized model the current is confined to the surface of a sphere of radius $r_0 = a/2$, with current per unit length $\mathbf{K}$. More realistically, the current is spread out over a shell of thickness δr within the Earth's core. Let $\mathbf{J}$ be the volume current density in that shell, which we may estimate as $\mathbf{J} \sim \mathbf{K}/\delta r$. If the current really is limited to a thin shell, with $\delta r \ll r_0$, then the current sheet model should be an accurate approximation. Even if δr is not very small, the current sheet model should provide a reasonable order-of-magnitude estimate of the power dissipated in Joule heating.

The power of Joule heating is I^2R where we estimate the current as $I \sim JA$ and the resistance as $R \sim \rho \ell / A$ where ρ is the resistivity. Here A and ℓ are the area and length, respectively, over which the current is spread. We estimate $A\ell$ as the volume $4\pi r_0^2 \delta r$ of the shell of current. Thus the power is

$$P \sim J^2 \rho A \ell \sim K^2 \rho \, \frac{4\pi r_0^2}{\delta r}. \tag{61}$$

The resistivity in the Earth's core is not known with accuracy, but geophysicists estimate that it is approximately $1.7 \times 10^{-6}\ \Omega$m. Using this value, as well as $r_0 = a/2 \sim 3 \times 10^6$ m and $\delta r \sim 10^5$ m, we estimate that the power dissipated in resistance is

$$P \sim 2 \times 10^9 \text{ W}. \tag{62}$$

This calculation is only meant to be an order-of-magnitude estimate. There are other estimates, based on more sophisticated models, of the power required to sustain the geodynamo. These fall in the range 10^{11}–10^{12} W but, because of unknowns in their underlying assumptions, the power is uncertain by one or two orders of magnitude. The source of this energy is another interesting question in geomagnetism.[25]

V. CONCLUDING REMARKS

One of the challenges of this work is how to visualize the results so that they are useful for instructional purposes. What makes this difficult is that the actual magnetic field and source currents are three dimensional and complicated. We have therefore shown these quantities on Mercator planes, which have the advantages of (a) two-dimensional representation, and (b) vector operations that are related to familiar ones. We suggest also that the adaptation of vectors in spherical coordinates, natural to the Earth, to the planar coordinates which are natural to Mercator projections, is itself pedagogically interesting.

We emphasize that the results for Earth's magnetic field, which are shown in Figs. 1–6, follow directly from the measured field[18,19] and Maxwell's equations for magnetostatics, (1). Figures 1–4 give the field over the surface and Figs. 5 and 6 give the internal field at half the Earth's radius, $r_0 = a/2$, which we have chosen for convenience. In calculating the results on Figs. 5 and 6 we assumed as an approximation that the current sources are within $a/2$. This is reasonable because the liquid outer core extends only to $0.55a$.

One of the unexpected results of this analysis is that the dipole character of the magnetic field at the surface of the Earth does not signify that the source of the field is itself characteristically dipolar. Rather, as Figs. 5 and 6 and Table II show, when one considers the field close to the source, there are large contributions from higher multipoles. In other words the surface field is dipolar because the surface is relatively remote from the sources.

The results for the current sources of Earth's magnetic field, which are shown in Figs. 7 and 8, are obtained by combining the observed field with our model of the sources. That model, which takes the currents to be confined to the surface of a sphere inside the Earth, is the simplest model of currents that can give the observed field. The actual source is a three-dimensional current density $\mathbf{J}(r, \theta, \phi)$, which is not yet known well although there are recent interesting computer models of it,[8,9] rather than the two-dimensional current $\mathbf{K}(\theta, \phi)$ of our model. But we should like to emphasize that the shape and magnitude of $\mathbf{K}$, as shown in Figs. 7 and 8, are related to the actual sources in that both give the observed field. The streamlines and currents in Figs. 7 and 8 are complicated because the actual currents are complicated. According to modern geophysical theory the source currents in the Earth are a self-exciting, self-maintaining dynamo. Cowling's theorem and other antidynamo theorems[26] show that these currents cannot be simple or symmetric.

[1] R. T. Merrill, M. W. McElhinny, and P. L. McFadden, *The Magnetic Field of the Earth* (Academic, San Diego, 1996).
[2] J. A. Jacobs, *Geomagnetism* (Academic, London, 1987), Vols. 1, 2, and 3.
[3] C. Kittel, *Introduction to Solid State Physics* (Wiley, New York, 1986), 6th ed.
[4] L. H. Kellogg, ''Mapping the Core-Mantle Boundary,'' Science **277**, 646 1997.
[5] R. Jeanloz and B. Romanowicz, ''Geophysical Dynamics at the Cener of the Earth,'' Phys. Today **50**, 22–27, August (1997).
[6] W. M. Elsasser, ''Hydromagnetism. I. A Review,'' Am. J. Phys. **23**, 590–609 (1955).
[7] G. Backus, ''Poloidal and toroidal fields in geomagnetic field modeling,'' Rev. Geophys. **24**, 75–109 (1986).

[8]G. A. Glatzmaier and P. H. Roberts, ''Rotations and magnetism of Earth's inner core,'' Science **274**, 1887–1891 (1996).
[9]W. Kuang and J. Bloxham, ''An Earth-like numerical dynamo model,'' Nature (London) **389**, 371–374 (1997).
[10]D. R. Stump and G. L. Pollack, ''Magnetic dipole oscillations and radiation damping,'' Am. J. Phys. **65**, 81–87 (1997).
[11]G. L. Pollack and D. R. Stump, ''Two magnets oscillating in each other's fields,'' Can. J. Phys. **75**, 313–324 (1997).
[12]D. R. Stump, G. L. Pollack, and J. Borysowicz, ''Magnets at the corners of polygons,'' Am. J. Phys. **65**, 892–897 (1997).
[13]D. R. Stump and G. L. Pollack, ''Radiation by a neutron in a magnetic field,'' Eur. J. Phys. **19**, 59–67 (1998).
[14]G. M. Julian and A. M. Stueber, ''Physicist+Geologist→Geophysics Course,'' Am. J. Phys. **42**, 556–559 (1974).
[15]J. A. Jacobs, *Reversals of the Earth's Magnetic Field* (Hilger, Bristol, 1984).
[16]S. Chapman and J. Bartels, *Geomagnetism* (Clarendon, Oxford, 1940).
[17]R. A. Langel, Chap. 4 in Vol. 1 of Ref. 2.
[18]C. E. Barton, Revision of International Geomagnetic Reference Field Released http:/www.ngdc.noaa.gov/seg/potfld/igrf95.html Copyright 1996 American Geophysical Union.
[19]Figure 2.2 in Ref. 1 shows the global distribution of the magnetic observatories which make the measurements from which IGRF coefficients are determined.
[20]J. D. Jackson, *Classical Electrodynamics* (Wiley, New York, 1975), 2nd ed.
[21]D. J. Griffiths, *Introduction to Electrodynamics* (Prentice–Hall, Englewood Cliffs, NJ, 1989), 2nd ed.
[22]E. J. Konopinski, *Electromagnetic Fields and Relativistic Particles* (McGraw–Hill, New York, 1981).
[23]Equation (3.70) of Ref. 20.
[24]S. Van Wyk, ''Problem: The energy contained in the Earth's magnetic field,'' Am. J. Phys. **54**, 121, 181 (1986).
[25]See, for example, Sec. 7.7 in Ref. 1.
[26]P. H. Roberts and D. Gubbins, Chap. 2, and P. H. Roberts, Chap. 3, in Vol. 2 of Ref. 2.